Dynamic Grid Deformation: Continuous Mapping Approach

Joseph M. Prusa[1] **and Piotr K. Smolarkiewicz**[2]

[1] *Iowa State University, Ames, Iowa, U.S.A.*
[2] *National Center for Atmospheric Research, Boulder, Colorado, U.S.A.*

ABSTRACT

Herein, we review our effort to date with the development of a deformable-coordinates multi-scale anelastic model. The model is designed using a synergetic interaction between the rules of continuous mapping and the strengths of nonoscillatory forward-in-time (NFT) numerical schemes. This approach leads to an efficacious computational model that is highly accurate and capable of simulating a wide variety of flows.

1. Introduction

Geophysical flows are generally characterized by enormous ranges of scales. An elementary example is provided by a convective atmospheric storm — where the scales of significant physical processes that occur range from water/ice droplet condensation/evaporation/sublimation $\sim 10^{-5}$ m to the outer convective dynamics of the storm $\sim 10^{5}$ m — a staggering ratio of ten billion to one. Effective parameterizations of the microphysical processes may eliminate the dependency upon sub-meter scales; however microphysical processes are known to depend sensitively upon local environmental conditions. From the simulation viewpoint the outstanding question is then just how finely must local environments be resolved? The answer depends in a complicated way upon the processes being simulated. For cloud parameterizations in regional to global atmospheric models, the minimum resolution may be cloud system-resolving $\sim 1km$ [20]. While this is well beyond current state of the art global simulations, advances in computational hardware and software will likely make such resolutions attainable in a reasonably-near future. We believe that mesh adaptivity should play a significant role in this development as well as in other high performance computations of geophysical problems.

With mesh adaptivity for simulating complex geophysical flows in mind, we have developed a generalized mathematical framework for the implementation of deformable coordinates in a generic Eulerian/semi-Lagrangian format of nonoscillatory-forward-in-time (NFT) schemes [19][34][29]. The key element of the framework is a time-dependent coordinate transformation, implemented rigorously throughout the governing equations of the nonhydrostatic anelastic model for simulating a broad range of idealized atmospheric/oceanic flows on scales from micro to planetary [28]. A computational model that is designed from the bottom up combining NFT algorithms and generalized coordinates is ideally suited for continuous grid adaptation. The robust performance of NFT methods enables the ability to mimic "nested" grids [19] and to accommodate large-amplitude undulations of the model boundaries [34][29]. Furthermore, since NFT methods offer a means of implicit subgrid-scale (SGS) modeling,[1] even an explicitly-inviscid model formulation can be quite effective in assuring a quality large-eddy-simulation (LES) of high Reynolds number geophysical flows [28]. Together with the momentum/velocity representation of the governing equations and the associated *discrete* elliptic problem, these properties facilitate turbulent-flow studies in generalized coordinates by obviating the task of evaluating the more cumbersome of the differential expressions such as vorticity, scalar Laplacian, and viscous stress.

[1] For a theoretical rationale and result analysis see [11] and [12][5], respectively.

Although not essential for simulating geophysical flows, rigorous and accurate representation of the vector differential calculus in generalized coordinates is important. The curl operator, $\nabla\times$, is required for accurate evaluation of vorticity/potential-vorticity budgets — a discriminating tool for analyzing complex vortical flows (see [21] for an example). The strain-rate tensor, $[\nabla\mathbf{v}+\nabla\mathbf{v}^T]$, is a key element of direct numerical simulation (DNS). Knowledge of its exact form in generalized coordinates allows one to extend the expertise of meteorological models to low Reynolds number flows, in the spirit of laboratory studies which often supplement research on the dynamics of atmospheres and oceans (e.g., [21][28][35]). Also, it is a key element of explicit SGS models that are useful, beyond standard LES studies, for diagnosing SGS fluctuations and flow uncertainties. Finally, because the curl and gradient operators emphasize important aspects of fluid flows, they may serve well as discriminating indicators for *driving* the grid adaptivity itself.

The fundamental differential operators have a tangible, physical existence that is independent of any coordinate-based description. However, coordinate-based representations are necessary for computing the explicit form of all requisite terms. Since the precise form of the terms depends upon the coordinate system being used, a tensor representation is preferable. The latter reveals [19] three distinct forms of velocity (physical, contravariant, and solenoidal) helpful for designing an efficient, high Reynolds number NFT fluid solver in generalized coordinates. Applications involving vorticity and/or strain rate also require consideration of the covariant form [29]. With the four distinct forms of velocity and numerous identities — which arise from the coordinate-invariance of geometric properties of the time-evolving physical domain — there are a number of various coordinate-dependent operator representations. Although they are all analytically equivalent, they lead to various numerical approximations that are not equally effective.

Herein, we review our effort to date with the development of a deformable-coordinates multi-scale anelastic model designed from the bottom up relying on the strengths of nonoscillatory transport methods. In the following section we outline the governing anelastic-model equations and summarize the computational approach. In section 3, we discuss extensions for curvilinear representation of the vorticity, Fickian diffusion, strain, and stress as well as tensor identities complementing the preceding development. Theoretical discussions are illustrated with examples of idealized flows. Remarks in section 4 conclude the paper.

2. Anelastic luid model in deformable coordinates

2.1 Motivation

For research studies of all-scale geophysical fluids — including nuances of coordinate transformations and associated numerical issues — we have found the anelastic nonhydrostatic system beneficial. Although the nonhydrostatic anelastic equations have been shown to be accurate for modeling the elements of weather and climate up to synoptic scale [17], their suitability for global weather and climate prediction has been often criticized — lately, using arguments of linear normal mode analysis [4]. Notwithstanding, our recent numerical results [27][8] document that the anelastic equations do adequately capture a range of idealized planetary flows. This has important practical consequences. Inherent in the anelastic system are (i) the Boussinesq linearization of the pressure gradient forces and the mass fluxes in the momentum and mass continuity equations, respectively, and (ii) the anelasticity *per se*, equivalent to taking the limit of an infinite speed of sound. Working in concert, these two approximations greatly simplify the design of second-order-accurate, flexible, and computationally efficient (viz., implicit with respect to inertia-gravity waves) research models for a broad range of geophysical flows. From the perspective of numerical engineering, the anelastic model code forms a basis of several other modeling systems, since it converts easily into either compressible/incompressible Boussinesq or incompressible Euler flow solvers [27], or even into a fully compressible solver for high-speed flows [30]. The rigor imposed by the associated boundary value problem for the anelastic pressure equation benefits the accuracy of the converted models.

2.2 Analytic Formulation

To address a broad class of geophysical flows in a variety of domains, — with, optionally, Dirichlet, Neumann, or periodic boundaries in each direction —we formulate (and solve) the governing equations in transformed coordinates $(\overline{t},\overline{x},\overline{y},\overline{z})$ within a computational domain $\mathbf{S}_t$ with, in general, cuboidal, toroidal, or a spheroidal topology implied by the physical boundary conditions. The coordinates (t,x,y,z) in the physical domain $\mathbf{S}_p$ are assumed orthogonal and stationary — Cartesian or spherical are typical examples. The physical domains admitted under the diffeomorphism

$$(\overline{t},\overline{x},\overline{y},\overline{z}) \equiv (\ t,\ E(t,x,y),\ D(t,x,y),\ C(t,x,y,z)\ )\ , \tag{1}$$

cover a range from the canonical Cartesian box, to spherical shells with irregular undulating boundaries. In the latter case, the topology of the cuboid is still an option. By removing an arbitrary small circle about the poles, the traditional differentiation across the pole is replaced with Neuman boundaries on the circle, thereby simplifying the use of the same model both for global and small-to-mesoscale applications. This option is important for improving communications in the massively-parallel variant of the model code when a grid deforms in the vicinity of the poles. The assumption in (1) that the transformed horizontal coordinates $(\overline{x},\overline{y})$ are independent of the vertical coordinate z follows the primary hydrostatic structure of the atmosphere and oceans and simplifies the metric terms. Examples of mappings embedded in (1) include the classical terrain-following coordinates of Gal-Chen and Somerville [7], their time dependent extensions [18][34], as well as a horizontal stretching whereby the horizontal coordinates in $\mathbf{S}_t$ are arbitrary (in theory subject to C^2 continuity; cf. [19]) functions of the time and horizontal coordinates in $\mathbf{S}_p$.

Given the transformation (1) the anelastic equations of Lipps and Hemler [9] can be written as follows

$$\frac{\partial(\rho^*\overline{v}^k)}{\partial\overline{x}^k} = 0\ . \tag{2}$$

$$\frac{dv^j}{d\overline{t}} = -\ \widetilde{G}^k_j\frac{\partial\pi'}{\partial\overline{x}^k} + g\frac{\theta'}{\theta_b}\delta_3{}^j + \mathscr{F}^j + \mathscr{V}^j\ , \tag{3}$$

$$\frac{d\theta'}{d\overline{t}} = -\overline{v}^k\frac{\partial\theta_e}{\partial\overline{x}^k} + \mathscr{H}\ , \tag{4}$$

where the physical and geometrical aspects intertwine each other. Insofar as the physics is concerned: v^j denotes components of the *physical velocity* (defined in $\mathbf{S}_p$);[2] θ, ρ, and π denote potential temperature, density, and a density-normalized pressure; g is the acceleration of gravity; $\mathscr{F}^j$ symbolizes the deviation of inertial forces (e.g., Coriolis and geospherical metric accelerations) from the geostrophically-balanced ambient (or environmental) state v^j_e, θ_e; whereas $\mathscr{V}^j$ and $\mathscr{H}$ symbolize viscous dissipation of momentum and diffusion of heat, respectively. Primes denote perturbations with respect to the environmental state, and the subscript $_b$ refers to the basic state, i.e., a horizontally homogeneous hydrostatic reference state of a Boussinesq type expansion around a constant stability profile (cf. section 2b in [3], for a discussion).

The geometry of the coordinates in (1) enters the governing equations as follows: $\rho^* := \rho_b\overline{G}$,[3] $\overline{G}$ denoting the Jacobian of the transformation (defined in the subsequent paragraph), and $j,k = 1,2,3$ correspond to "x", "y", "z" components, respectively, in either $\mathbf{S}_p$ or $\mathbf{S}_t$. In the momentum equation (3), $\widetilde{G}^k_j := \sqrt{g^{jj}}(\partial\overline{x}^k/\partial x^j)$ are renormalized elements of the Jacobi matrix where summation is not implied over j, and $\delta_3{}^j$ is the Kronecker delta. The coefficients g^{jj} are the diagonal elements of the conjugate metric tensor of $\mathbf{S}_p$ (defined below). The

[2] In meteorological applications, the physical velocity is typically defined using a local Cartesian system and so has dimensions of length/time; a distinct representation of the physical velocity, $\overline{v}^j \neq v^j$, also exists for the transformed coordinate system; cf. [19].

[3] We use := to mean *defined as*, to distinguish from ≡ (*identically*).

total derivative is given by $d/d\overline{t} = \overline{v^*}^i(\partial/\partial\overline{x}^i)$, where $\overline{v^*}^i := d\overline{x}^i/d\overline{t} := \dot{\overline{x}}^i$ is the *contravariant velocity* in $\mathbf{S}_t$. Here $i = 0,1,2,3$; and $i = 0$ refers to time $\overline{t}$. Appearing in the mass continuity (2) and potential temperature (4) equations is the *solenoidal velocity*,

$$\overline{v^s}^k := \overline{v^*}^k - \frac{\partial \overline{x}^k}{\partial t} \,. \tag{5}$$

so named for distinction, because of the form mass continuity takes with it. This solenoial form readily follows — given $\rho_b = \rho_b(\mathbf{x})$, and the time-independent coordinate system in $\mathbf{S}_p$ — from the tensor invariant form of anelastic mass continuity equation $\overline{G}^{-1}\partial(\rho_b \overline{G}\overline{v^*}^i)/\partial\overline{x}^i \equiv 0$ see [19] and the references therein for a discussion.[4] Since the identity transformation is specified for the time coordinate (1), the solenoidal velocity for the time coordinate vanishes, i.e., $\overline{v^s}^0 \equiv 0$. For this reason the indices in (5) indicate the usual three spatial elements, whereas the contravariant velocity is defined more generally as a 4-element 1-form (1-forms have one index, 2-forms have 2 indices,...). Use of the solenoidal velocity facilitates the solution procedures because it preserves the incompressible character of numerical equations. While numerous relationships can be derived that express any velocity (solenoidal, contravariant, or physical) in terms of the other, in either transformed or physical coordinate system [19], a particularly useful transformation

$$\overline{v^s}^j = \widetilde{G}^j_k v^k \,. \tag{6}$$

relates the solenoidal and physical velocities directly.

The elements of the metric tensor of the transformed coordinates are $\overline{g}_{mn} = g_{pq}(\partial x^p/\partial\overline{x}^m)\cdot(\partial x^q/\partial\overline{x}^n)$, where g_{pq} denotes the metric tensor of the physical coordinate system (which need not be Cartesian). The Jacobian is then $\overline{G} = |\overline{g}_{mn}|^{1/2}$. The elements of g_{pq} may be computed from the definition of the fundamental metric $ds^2 = g_{pq}dx^p dx^q$ by employing geometrical arguments. In particular, for $\mathbf{S}_p$ with orthogonal coordinates, the Pythagorean Theorem may be used to construct ds^2 within an infinitesimal volume element. The elements of the conjugate metric tensor, needed in (3), are then computed from $g^{jj} = 1/g_{jj}$ since $g_{pq} = 0$ for $p \neq q$.[5] Note that unlike g^{pq}, the metric coefficients $\widetilde{G}^q_p$ appearing in Eq.'s (3) and (6) are *not* symmetric (i.e., $\widetilde{G}^q_p \neq \widetilde{G}^p_q$).

2.3 Numerical Approximations

Given (2), each prognostic equation of the anelastic system (3) and (4) can be written compactly either as a Lagrangian evolution equation

$$\frac{d\psi}{d\overline{t}} = R \,, \tag{7}$$

or an Eulerian conservation law

$$\frac{\partial \rho^* \psi}{\partial \overline{t}} + \overline{\nabla}\bullet(\rho^* \overline{\mathbf{v}}^* \psi) = \rho^* R \,. \tag{8}$$

Here ψ symbolizes v^j or θ', R denotes the associated rhs, $\overline{\nabla}\bullet := \partial/\partial\overline{\mathbf{x}}$,[6] where $\overline{\mathbf{x}} := (\overline{x}, \overline{y}, \overline{z})$.

The theory and performance of our NFT approach have been broadly documented in the literature; see [28] for a succint review. In essence, we approximate either (8) or (7) to second-order accuracy in space and time,

[4] Note that the tensor invariant form has a time derivative even though the anelastic approximation is being used, a result of the time variation of the geometry of $\mathbf{S}_t$ in (1).

[5] In choices of $\mathbf{S}_p$ with non-orthogonal coordinates, the metric tensor can be computed analytically from its definition, given a mapping from a coordinate system with known metric structure to the non orthogonal one. The conjugate metric tensor can be determined from $g_{pk}g^{kq} \equiv \delta^q_p$.

[6] This divergence operator as well as the gradient operator defined for (10) —(12) are compact notations useful for conveying the structure of the numerical operators; although similar to the tensor invariant forms of divergence and gradient which appear in subsequent sections, they are devoid of the metric structure of $\mathbf{S}_t$.

employing a formal congruency of the Eulerian [24] and semi-Lagrangian [23] optional model algorithms, respectively. Then either algorithm can be written in the compact form

$$\psi_{\mathbf{i}}^{n+1} = LE_{\mathbf{i}}(\tilde{\psi}) + 0.5\Delta t R_{\mathbf{i}}^{n+1} := \widehat{\psi}_{\mathbf{i}} + 0.5\Delta t R_{\mathbf{i}}^{n+1} ; \tag{9}$$

where $\psi_{\mathbf{i}}^{n+1}$ is the solution sought at the grid point $(\bar{t}^{n+1}, \overline{\mathbf{x}}_{\mathbf{i}})$, $\tilde{\psi} := \psi^n + 0.5\Delta t R^n$, and LE denotes a two-time-level either advective semi-Lagrangian or flux-form Eulerian NFT transport operator. In the Eulerian scheme, LE integrates the homogeneous transport equation (8), i.e., LE advects $\tilde{\psi}$ using a fully second-order-accurate multidimensional NFT advection scheme [25][28]; whereas in the semi-Lagrangian algorithm, LE remaps transported fields, which arrive at the grid points $(\bar{t}, \overline{\mathbf{x}}_{\mathbf{i}})$, back to the departure points of the flow trajectories $\left(\bar{t}^n, \overline{\mathbf{x}}_o(\bar{t}^{n+1}, \overline{\mathbf{x}}_{\mathbf{i}})\right)$ also using NFT advection schemes [22][23].

For inviscid adiabatic flows, equation (9) represents a system of equations that is implicit with respect to all dependent variables in (3) and (4), since all forcing terms are assumed to be unknown at $n+1$. For the physical velocity vector $\mathbf{v} = [v^1, v^2, v^3]$, it can be written compactly as

$$\mathbf{v}_{\mathbf{i}} = \widehat{\mathbf{v}}_{\mathbf{i}} - 0.5\Delta t \left(\widetilde{\mathbf{G}}(\overline{\nabla}\pi')\right)_{\mathbf{i}} + 0.5\Delta t \mathbf{R}_{\mathbf{i}}(\mathbf{v}, \widehat{\theta}) , \tag{10}$$

where $\widetilde{\mathbf{G}} \equiv \left[\widetilde{G}_j^k\right]$ with the matrix elements $\widetilde{G}_j^k$ defined in section 2.2, $\forall_\zeta \ \overline{\nabla}\zeta := \partial\zeta/\partial\overline{\mathbf{x}}$ (see footnote 6), and $\mathbf{R}_{\mathbf{i}}(\mathbf{v}, \widehat{\theta})$ accounts for the implicit representation of the buoyancy via (4). On grids unstaggered with respect to all prognostic variables (e.g., A and B Arakawa grids), (10) can be inverted algebraically to construct expressions for the solenoidal velocity components that are subsequently substituted into (2) to produce

$$\left\{\frac{\Delta t}{\rho^*}\overline{\nabla} \bullet \rho^* \widetilde{\mathbf{G}}^T \left[\left(\mathbf{I} - 0.5\Delta t \mathbf{R}\right)^{-1}\left(\widehat{\mathbf{v}} - 0.5\Delta t \widetilde{\mathbf{G}}(\overline{\nabla}\pi')\right)\right]\right\}_{\mathbf{i}} = 0 ; \tag{11}$$

that is, an elliptic equation for pressure

$$\left\{\frac{\Delta t}{\rho^*}\overline{\nabla} \bullet \rho^* \widetilde{\mathbf{G}}^T \left[\widehat{\widehat{\mathbf{v}}} - \left(\mathbf{I} - 0.5\Delta t \mathbf{R}\right)^{-1} \widetilde{\mathbf{G}}(\overline{\nabla}\pi'')\right]\right\}_{\mathbf{i}} = 0 , \tag{12}$$

where $\widehat{\widehat{\mathbf{v}}} - \left(\mathbf{I} - 0.5\Delta t \mathbf{R}\right)^{-1} \widetilde{\mathbf{G}}(\overline{\nabla}\pi'') \equiv \overline{\mathbf{v}}^s$ defined in (5), $\pi'' := 0.5\Delta t \pi'$; cf. [19] for the complete development. Boundary conditions imposed on $\overline{\mathbf{v}}^s \bullet \overline{\mathbf{n}}$, subject to the integrability condition $\int_\Omega \rho^* \overline{\mathbf{v}}^s \bullet \overline{\mathbf{n}} d\sigma = 0$, imply the appropriate boundary conditions on π'' [19, 34]. Here $\Omega = \partial \mathbf{S}_t$ and $\overline{\mathbf{n}} d\sigma$ is the corresponding area element with local orientation perpendicular to Ω. The resulting boundary value problem is solved using a preconditioned nonsymmetric Krylov-subspace solver [26]. Given the updated pressure, and hence the updated solenoidal velocity, the updated physical and contravariant velocity components are constructed from the solenoidal velocities using transformations (6) and (5), respectively. Nonlinear terms in R^{n+1} (e.g., metric terms arising on the globe) may require outer iteration of the system of equations generated by (9) [27]. When included, diabatic, viscous, and subgrid-scale forcings may be first-order-accurate and explicit, e.g., assume $SGS(\psi^{n+1}) = SGS(\psi^n) + \mathcal{O}(\Delta t)$ in R^{n+1}, see section 3.5.4 in [25]. For extensions to moist processes, see [8].

3. Extensions

3.1 Vorticity

The vorticity, defined as the curl of the velocity field $\boldsymbol{\omega} = \nabla \times \mathbf{v}$, carries physical significance independent of the choice of coordinate system that one uses to describe a fluid flow. In curvilinear coordinates, one needs to carefully distinguish between covariant and contravariant (as well as mixed) forms in order that a *physical* vorticity with *appropriate* dimensions may be recovered, for this is what one would observe in a laboratory or in the field.

Following the notation of the preceding section, we begin with the formal definition of vorticity in the coordinate-invariant covariant tensor form, cf. [31]:

$$\overline{\omega}^*{}_{jk} = \overline{v}^*{}_{k,j} - \overline{v}^*{}_{j,k} \,. \tag{13}$$

Here $\overline{v}^*{}_j$ denotes the covariant velocity distinguished from the contravariant velocity $\overline{v}^j$ only by the index position[7], and indices following a comma refer to covariant differentiation; i.e., evaluating elements of the gradient operator. In particular, for the covariant velocity

$$\overline{v}^*{}_{j,k} = \frac{\partial \overline{v}^*{}_j}{\partial \overline{x}^k} - \overline{\left\{ \begin{matrix} p \\ j\ \ k \end{matrix} \right\}} \overline{v}^*{}_p \,. \tag{14}$$

The term in brackets is a Christoffel symbol of the second kind [31], and it appears due to the twisting and turning of the curvilinear coordinates. It may be computed from:

$$\overline{\left\{ \begin{matrix} p \\ j\ \ k \end{matrix} \right\}} = \overline{g}^{pq} \left[\frac{1}{2} \left(\frac{\partial \overline{g}_{jq}}{\partial \overline{x}^k} + \frac{\partial \overline{g}_{kq}}{\partial \overline{x}^j} - \frac{\partial \overline{g}_{jk}}{\partial \overline{x}^q} \right) \right]. \tag{15}$$

The term in square brackets is a Christoffel symbol of the first kind, and is denoted as $[jk,q]$ [31]. Similar to j,k, the indices $p,q = 1,2,3$ correspond to "x", "y", and "z". Equation (15) reveals that both types of Christoffel symbols are symmetric with respect to indices (j,k). Because of this symmetry, when (14) is substituted into (13), the Christoffel terms cancel and the derivatives appearing in (13) may be interpreted as partial derivatives. However we retain the definition using covariant derivatives since in general partial derivatives do not correspond to tensor forms.

The covariant vorticity (13) is the principal form. However, we wish to develop the physical vorticity form as a function of physical velocity gradients. In general covariant velocities are unavailable in the model, because they are not required to solve the governing equations. Routinely stored are the physical velocity components v^j expressed in terms of the coordinates $\overline{\mathbf{x}}$ of the transformed space $\overline{\mathbf{S}}$ where the computation is done. In order to compute in $\mathbf{S}_t$ the physical vorticity defined in $\mathbf{S}_p$ in terms of v^j we (i) write (13) for the reference system $\mathbf{S}_p$ using the covariant velocities of the reference system $v^*{}_j$, (ii) rewrite the covariant velocities in terms of the physical velocities using $v^*{}_j = \sqrt{g_{jj}}\, v^j$, (iii) transform all spatial derivatives into the curvilinear space $\overline{\mathbf{S}}$ using the chain rule, and (iv) extract the physical vorticity by rescaling according to $\omega^*{}_{jk} = \sqrt{g_{jj} g_{kk}}\, \omega^{jk}$. The final result is:

$$\omega^{jk} = \sqrt{g^{kk}}\, \widetilde{G}^p_j \frac{\partial \sqrt{g_{kk}}\, v^k}{\partial \overline{x}^p} - \sqrt{g^{jj}}\, \widetilde{G}^q_k \frac{\partial \sqrt{g_{jj}}\, v^j}{\partial \overline{x}^q} \,. \tag{16}$$

Although this expression appears considerably more complicated than (13), our restriction to orthogonal coordinate systems for $\mathbf{S}_p$ has resulted in a relatively simple expression. The simplification occurs in the conversions from covariant to physical forms, which more generally (for non-orthogonal coordinates) are $v^*{}_j = (g_{jp}/\sqrt{g_{pp}})\, v^p$ for the velocity, and $\omega^*{}_{jk} = \sqrt{g_{jj}/g_{pp}}\; g_{kp}\, \omega^{jp}$ for the vorticity. Unlike the orthogonal conversions used in (16), these more general forms involve a repeating index p [1]. Note that the covariant form (13) and *not* the physical form (16) is a coordinate invariant tensor form of vorticity. The covariant form is much simpler, is already written in conservative form, and will be shown to exhibit the expected symmetries with the rate of strain tensor in section 3.3. An immediate observation from equations (13-15) is that $\overline{\omega}^*{}_{jk}$ is skew symmetric. Thus any three independent elements suffice to describe the vorticity *vector* (e.g., we could define $\omega^x = \omega_{23}$, $\omega^y = \omega_{31}$, and $\omega^z = \omega_{12}$). With this structure in mind, (16) may be written more compactly as:

$$\omega^q = \varepsilon_{qjk} \sqrt{g^{kk}}\, \widetilde{G}^p_j \frac{\partial \sqrt{g_{kk}}\, v^k}{\partial \overline{x}^p} \,, \tag{17}$$

[7] In any coordinate system, $\overline{v}^*{}_k = \overline{g}_{jk}\, \overline{v}^{*\,j}$, an operation termed the *lowering* of indices.

where ε_{qjk} is the permutation symbol.

Another derivation of interest involves the divergence of the vorticity, $\nabla \bullet \boldsymbol{\omega} = \nabla \bullet \nabla \times \mathbf{v} \equiv 0$, a fundamental vector differential identity. Since we compute the divergence, the vorticity must be expressed in contravariant form (see section 3.2, equations (26- 28) for the development of the generalized divergence operator). This is readily accomplished using (13-17). The key elements are to (i) convert (17) into a contravariant-like form using $\omega^{*q} = \sqrt{g^{qq}}\,\omega^q$, and (ii) utilize (13) and (14), both written for $\mathbf{S}_p$, to reorganize the rescaled version of (17) into the proper tensor form. One then obtains the alternate, contravariant vector form of vorticity:

$$\omega^{*q} = \varepsilon^{*qjk} v^*_{k,j}. \tag{18}$$

Here $\varepsilon^{*qjk} := \varepsilon_{qjk}\sqrt{g^{qq}g^{jj}g^{kk}} \equiv \varepsilon_{qjk}G^{-1}$ is the third order, contravariant permutation *tensor* [1], and G is the Jacobian for $\mathbf{S}_p$. Using equation (28) the tensor invariant form for the divergence of the vorticity vector is then defined to be:

$$\nabla \bullet \boldsymbol{\omega} := \frac{1}{G}\frac{\partial}{\partial x^q}\left(G\varepsilon^{*qjk} v^*_{k,j}\right) \equiv 0. \tag{19}$$

That this expression is indeed indentically zero may be determined by direct computation (expansion). Although (19) and it's analogue in $\mathbf{S}_t$ are analytically correct, neither is a form that is convenient for numerical computation. In order to construct a useful expression for the divergence of the vorticity, we begin with (19) but emphasize the physical vorticity components as given in (17). The chain rule is then utilized to transform derivatives into the coordinates of $\mathbf{S}_t$, and the resulting expression is rearranged as follows:

$$0 \equiv \frac{1}{G}\frac{\partial}{\partial x^q}\left(G\sqrt{g^{qq}}\omega^q\right) = \frac{1}{\overline{G}}\left(\frac{\overline{G}}{G}\frac{\partial \overline{x}^p}{\partial x^q}\right)\frac{\partial}{\partial \overline{x}^p}\left(G\sqrt{g^{qq}}\omega^q\right), \tag{20}$$

which is further rearranged into:

$$0 \equiv \frac{1}{\overline{G}}\frac{\partial}{\partial \overline{x}^p}\left\{\left(\frac{\overline{G}}{G}\frac{\partial \overline{x}^p}{\partial x^q}\right)\left(G\sqrt{g^{qq}}\omega^q\right)\right\} - \left(\frac{G\sqrt{g^{qq}}\omega^q}{\overline{G}}\right)\frac{\partial}{\partial \overline{x}^p}\left(\frac{\overline{G}}{G}\frac{\partial \overline{x}^p}{\partial x^q}\right). \tag{21}$$

The last term in (21) is identically zero via the tensor identity termed the *generalized conservation law* or GCL (see the discussion of (48) in Section 3.4). We simplify the remaining term by defining the *solenoidal* vorticity, $\overline{\omega^s}^p := \widetilde{G}^p_q \omega^q$, by analogy with the solenoidal velocity (6). The final result is:

$$\frac{1}{\overline{G}}\frac{\partial}{\partial \overline{x}^p}\left(\overline{G}\,\overline{\omega^s}^p\right) \equiv 0. \tag{22}$$

Of considerable significance is that "other" expressions for the divergence of vorticity — for example using covariant, physical, or mixed forms inappropriately; and/or using divergence/curl "operators" without the correct metric structure *will not* satisfy the vector identity. In particular, if a non-Cartesian coordinate system is used to describe $\mathbf{S}_p$, then the physical velocity/vorticity components are not the correct forms to enter directly into the curl/divergence operators.

Finally we consider how to compute Ertel's potential vorticity, $P = (\boldsymbol{\omega} \bullet \nabla\theta)/\rho_b$. For adiabatic, frictionless flows, P is a conserved quantity, i.e., $dP/dt \equiv 0$ [2], making it a valuable tracer for dynamical studies. Since P is a scalar field, and $\nabla\theta$ is a pure covariant form, then $\boldsymbol{\omega}$ must be written in contravariant form. Thus:

$$P := \frac{\omega^{*j}}{\rho_b}\frac{\partial \theta}{\partial x^j} \equiv \frac{\overline{\omega^s}^j}{\rho_b}\frac{\partial \theta}{\partial \overline{x}^j} \tag{23}$$

The expression on the extreme right hand side gives a computationally useful form and follows immediately from the middle form of (23) when one rescales the contravariant vorticity into the physical vorticity, applies the chain rule to transform to the coordinates of $\mathbf{S}_t$, and organizes the resulting terms into the solenoidal vorticity as defined in (22).

In order to illustrate (17) and (22) at work, we consider the numerical simulation, presented in [34], of a flow of an ideal 3D homogeneous Boussinesq fluid past oscillating membranes. The membranes form impermeable free-slip upper and lower boundaries, Fig. 1, and their shape is prescribed, respectively, as

$$z_s(r(x,y),t) = \begin{cases} z_{s0}\cos^2(\pi r/2L)\sin(2\pi t/T) & \text{if } r/L \le 1, \\ 0 & \text{otherwise}, \end{cases} \tag{24}$$
$$H(x,y,t) = H_0 - z_s(x,y,t)\ ,$$

with $r = \sqrt{x^2+y^2}$, oscillation period $T = 48\Delta t$, amplitude $z_{s0} = 51.2\Delta z$, the membranes' half-width $L = 51.2\Delta x$, where $\Delta x = \Delta y = \Delta z$, and $C(t,x,y,z) = H_0\,(z-z_s)/(H-z_s)$ in (1). The computational domain consists of $160\times160\times128$ grid intervals, in the horizontal and vertical, respectively; and the LE operator in (9) is semi-Lagrangian. The domain deformation is significant, since at $t = T/4$, the upper and lower boundaries are separated merely by one fifth of the vertical extent of the model. The magnitude of the induced flow and its variation is approximately 5 and 0.5, respectively, as measured by $\mathscr{C} \equiv \| \Delta t\overline{\mathbf{v}}^*/\Delta\overline{\mathbf{x}} \|$ and $\mathscr{L} \equiv \| \Delta t\partial\overline{\mathbf{v}}^*/\partial\overline{\mathbf{x}} \|$ — the (maximal) Courant and "Lipschitz" numbers (cf. [23] for a discussion).

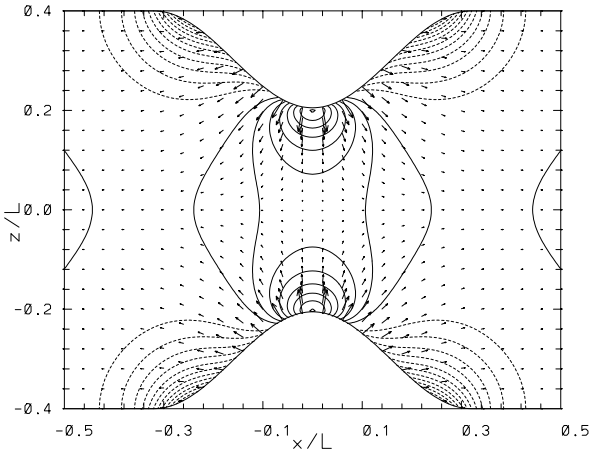

Figure 1: Potential flow simulation past 3D undulating boundaries. Flow vectors and isobars are shown in the central xz plane.

Table 1: Vorticity errors in a potential flow simulation

field	Max $\lvert . \rvert$	Average	Standard deviation
$\Delta t\omega^1$	$6.99\cdot10^{-2}$	$-4.87\cdot10^{-18}$	$1.90\cdot10^{-3}$
$\Delta t\omega^2$	$6.98\cdot10^{-2}$	$-3.19\cdot10^{-17}$	$1.90\cdot10^{-3}$
$\Delta t\omega^3$	$7.62\cdot10^{-3}$	$2.20\cdot10^{-18}$	$1.71\cdot10^{-4}$
$\Delta t\nabla\bullet\boldsymbol{\omega}^s$	$2.94\cdot10^{-5}$	$-7.52\cdot10^{-18}$	$3.75\cdot10^{-7}$

Lacking diabatic forces, boundary friction, and buoyancy, the experimental setup implies a potential-flow solution with zero integral pressure force on the bounding walls (D'Alembert paradox, cf. [14]). Indeed, the authors have verified in [34] that the pressure drag is on the order of round-off errors. We have computed $\boldsymbol{\omega}\Delta t$ as implied by (17), using standard centered finite-difference approximations. Since the simulated flow is clearly potential, the residual vorticity is primarily due to the truncation error of evaluating (17) itself. In general, we find the domain averaged residual vorticity($\times\Delta t$) on the order of round-off errors, with standard deviations $\lesssim 2\cdot10^{-3}$ — i.e., 3 and 2 orders smaller than the flow magnitude as measured, respectively, by $\mathscr{C}$ and $\mathscr{L}$. Furthermore, divergence of the solenoidal vorticity, evaluated from (22), is 7 and 6 orders smaller than $\mathscr{C}$ and $\mathscr{L}$. Thus our numerical results satisfy the vector identity for the vanishing of the divergence of curl to a high level of accuracy.[8] For emphasis, Table 1 shows statistics from $t = T/4$ when the displacement of

[8] The residual of the divergence of curl depends upon the level of pressure convergence.

membranes is maximal but flow weak ($\mathscr{C} = 1.2$ and $\mathscr{L} = 0.14$) thereby representing the worst-case scenario.

3.2 Scalar Diffusion

Scalar diffusion is of paramount importance in many geophysical processes, ranging from the transport of water vapor in the atmosphere to salt in the oceans and heat in both. We begin the generalized formulation by considering an arbitrary scalar field ϕ with diffusion flux proportional to the gradient of ϕ, defined in $\mathbf{S}_p$ as

$$\Phi^*_j := \rho_b \alpha \phi_{,j} \,. \tag{25}$$

Here α is a diffusivity coefficient (with the dimension length$^2\times$time^{-1}), and $\phi_{,j}$ denotes the partial derivative[9] with respect to x^j. Note that the flux Φ^*_j is a pure covariant form.

In order to compute the "$\rho_b\alpha$-modified Laplacian" of ϕ, $\mathscr{L}(\phi)$, we take the divergence of Φ^*_j, first *raising* it's index [31], since the argument for the generalized divergence operator must be a contravariant form. The divergence of $\Phi^{*j} = g^{jk}\Phi^*_k$ is defined to be the covariant derivative of Φ^{*j} contracted on j [1], i.e., $\Phi^{*j}_{,j}$. Thus $\mathscr{L}(\phi) := \Phi^{*j}_{,j}$ where

$$\Phi^{*j}_{,j} = \frac{\partial \Phi^{*j}}{\partial x^j} + \left\{ \begin{array}{cc} j \\ j & k \end{array} \right\} \Phi^{*k} \,. \tag{26}$$

The difference in sign of the Christoffel term compared to (14) is due to taking the covariant derivative of a contravariant form rather than a covariant form. It is possible to eliminate the Christoffel term in (26) and rewrite the divergence in conservative form by employing the identity

$$\left\{ \begin{array}{cc} j \\ j & k \end{array} \right\} \equiv \frac{1}{G}\frac{\partial G}{\partial x^k} \,, \tag{27}$$

cf. section 2.5 in [31]. Thus we may write the divergence as:

$$\Phi^{*j}_{,j} = \frac{1}{G}\frac{\partial G \Phi^{*j}}{\partial x^j} \,, \tag{28}$$

and the Laplacian as:

$$\mathscr{L}(\phi) = \frac{1}{G}\frac{\partial}{\partial x^j}\left(\alpha \rho_b g^{jj} G \frac{\partial \phi}{\partial x^j}\right) \,, \tag{29}$$

The scalar advection-diffusion equation can now be readily generalized from its typical form in Cartesian coordinates to the orthogonal coordinates of $\mathbf{S}_p$. Using (29), it must be:

$$\frac{d\phi}{dt} = S_\phi + \frac{1}{\rho_b G}\frac{\partial}{\partial x^j}\left(\alpha \rho_b g^{jj} G \frac{\partial \phi}{\partial x^j}\right) \,, \tag{30}$$

where the scalar field S_ϕ accounts for sources/sinks. The total derivative on the left hand side of (30) is in fact the material derivative when the transported field is a scalar. It is also an invariant form as revealed by:

$$\frac{d\phi}{dt} := \frac{\partial \phi}{\partial x^i} v^{*i} = \frac{\partial \phi}{\partial \overline{x}^m}\frac{\partial \overline{x}^m}{\partial x^i} v^{*i} = \frac{\partial \phi}{\partial \overline{x}^m}\overline{v}^{*m} =: \frac{d\phi}{d\overline{t}} \,. \tag{31}$$

The range of index $m = 0,1,2,3$ is the same as that of i; note that given the identity transformation for time in (1), that $v^{*0} = 1$. Equation (30) is not quite the fully generalized invariant form required for $\mathbf{S}_t$. The total derivative may be immediately rewritten in terms of $\mathbf{S}_t$ given (31). The Laplacian is transformed using exactly

[9] The notation of the previous section suggests that it is the *covariant* derivative that is needed here. In principle this is correct, however for the scalar field ϕ the contribution from Christoffel terms vanish, and one is left only with the partial derivative.

the same procedure as was used for the divergence of the vorticity, cf. equations (20) and (21), i.e., starting with (29), we employ the chain rule to change coordinates and reorganize as:

$$\overline{\mathscr{L}}(\phi) = \frac{1}{\overline{G}}\frac{\partial}{\partial \overline{x}^p}\left\{\left(\frac{\overline{G}}{G}\frac{\partial \overline{x}^p}{\partial x^j}\right)\left(\alpha\rho_b g^{jj} G\frac{\partial x^q}{\partial x^j}\frac{\partial \phi}{\partial \overline{x}^q}\right)\right\} - \frac{1}{\overline{G}}\left(\alpha\rho_b g^{jj} G\frac{\partial \phi}{\partial x^j}\right)\frac{\partial}{\partial \overline{x}^p}\left(\frac{\overline{G}}{G}\frac{\partial \overline{x}^p}{\partial x^j}\right) . \tag{32}$$

As in (21), we note that the second term on the right hand side of (32) vanishes because of the GCL (48). Recognizing the metric tensor element $\overline{g}^{pq}$ among the remaining coefficients in the first term yeilds:

$$\overline{\mathscr{L}}(\phi) = \frac{1}{\overline{G}}\frac{\partial}{\partial \overline{x}^p}\left(\alpha\rho^* \overline{g}^{pq}\frac{\partial \phi}{\partial \overline{x}^q}\right) , \tag{33}$$

Substituting (31) and (33) into (30), one obtains the generalized form:

$$\frac{d\phi}{d\overline{t}} = S_\phi + \frac{1}{\rho^*}\frac{\partial}{\partial \overline{x}^j}\left(\alpha\rho^* \overline{g}^{jk}\frac{\partial \phi}{\partial \overline{x}^k}\right) , \tag{34}$$

The source S_ϕ does not require any modification. This is the coordinate invariant form of the advection-diffusion equation, and since ϕ is a scalar, it is simultaneously in physical form.

The diffusion of heat, symbolized by the $\mathscr{H}$ term on the rhs of (4), is a particular realization of the general problem for scalar diffusion in (34). It is defined in $\mathbf{S}_p$ as a divergence of the diffusion flux of the scalar field θ'. Consequently,

$$\mathscr{H} = \frac{1}{\rho^*}\frac{\partial}{\partial \overline{x}^j}\left(\alpha\rho^* \overline{g}^{jk}\frac{\partial \theta'}{\partial \overline{x}^k}\right) , \tag{35}$$

thereby expressing $\mathscr{H}$ solely in $\mathbf{S}_t$, cf. [7].

3.3 Momentum Dissipation

Our use of a curvilinear, though orthogonal and stationary, reference space represents a significant departure from earlier transformation methods (e.g., [33][7]) where all relevant formulae were derived assuming Cartesian $\mathbf{S}_p$. Although our strategy — merely optional for Euclidean spaces — greatly simplifies designing all-scale models for geophysical flows, it calls for rederiving all relevant formulae. This is particularly tedious for the $\mathscr{V}^j$ term on the rhs (3).

The derivation of the viscous stress starts with the development of the strain rate tensor. Forthcoming from geometric principles, we begin by defining the *relative* strain rate tensor, ε'_{jk} in terms of the time rate of change of distance elements when co-moving with the flow. In the co-moving coordinates, denoted by x'^j, the relative strain rate tensor is defined by:

$$\varepsilon'_{jk} dx'^j dx'^k := \frac{1}{2}\frac{\mathscr{D}}{\mathscr{D}t'}\left(ds'^2\right) . \tag{36}$$

Here the operator $\mathscr{D}/\mathscr{D}t'$ denotes the time rate of change while keeping the co-moving coordinates x'^j constant; and is known as the *convected* derivative [1], [16]. This time derivative is distinct from the total (see (31) in section 3.2) and material derivatives (see (46) in section 3.4) that are formulated independently of any particular system of coordinates. Assuming $ds'^2 = g'_{jk} dx'^j dx'^k$, the metric tensor in co-moving coordinates contains all required information about the internal kinematics of fluid elements. Given this fundamental metric, (36) may be rewritten as

$$\varepsilon'_{jk} \equiv \frac{1}{2}\frac{\mathscr{D}}{\mathscr{D}t'}\left(g'_{jk}\right) . \tag{37}$$

It remains to transform this expression into the coordinates of $\mathbf{S}_t$. The transformation for the convected derivative is more involved than that for the material derivative because one must also include covariant derivatives of the velocity to account for the shift from co-moving coordinates. Following [1],[16],

$$\overline{\varepsilon}^*_{jk} \equiv \frac{1}{2}\left(\overline{g}_{jk,i}\overline{v}^{*\,i} + \overline{g}_{jm}\overline{v}^{*\,m}_{\ \ ,k} + \overline{g}_{nk}\overline{v}^{*\,n}_{\ \ ,j}\right) \ . \tag{38}$$

The first term on the right hand side includes the covariant derivative of the metric tensor — it is identically zero by *Ricci's lemma* [1]. Note this lemma implies that the metric tensor can be treated as a constant with regards to covariant differentiation. The remaining two terms can then be rearranged, e.g. $\overline{g}_{jm}\overline{v}^{*m}_{\ \ ,k} \equiv \left(\overline{g}_{\ jm}\overline{v}^{*m}\right)_{,k}$. The parenthetical term in this expression is simply the covariant velocity, thus we write the principle form of the strain rate tensor as:

$$\overline{\varepsilon}^*_{\ jk} \equiv \frac{1}{2}\left(\overline{v}^*_{\ k,j} + \overline{v}^*_{\ j,k}\right) \ , \tag{39}$$

the symmetric complement of the *rotation* (viz. half of the vorticity in Eq. 13) to the gradient of the covariant velocity. These are the *objective* forms (viz. observer independent [15]). An important observation to make about this form is that it is covariant; i.e., geometric considerations lead to the conclusion that the strain rate tensor should be defined as a 2-form covariant tensor. In order to compute the covariant strain rate components, (39) is (i) written for $\mathbf{S}_p$, (ii) (14) is used to expand the covariant derivatives, (iii) the covariant velocities are rescaled into the physical velocities, and (iv) the chain rule is used to rewrite the derivatives in terms of $\mathbf{S}_t$. The final result is:

$$\varepsilon^*_{jk} \equiv \frac{1}{2}\left(\sqrt{g_{jj}}\,\widetilde{G}^p_j\frac{\partial\sqrt{g_{kk}}v^k}{\partial\overline{x}^p} + \sqrt{g_{kk}}\,\widetilde{G}^q_k\frac{\partial\sqrt{g_{jj}}v^j}{\partial\overline{x}^q}\right) - \sqrt{g_{mm}}\left\{\begin{matrix} m \\ j\ \ k\end{matrix}\right\}v^m \ . \tag{40}$$

If needed, this expression may be rescaled to yield the physical strain rate, $\varepsilon^{jk} \equiv \sqrt{g^{jj}g^{kk}}\varepsilon^*_{jk}$. Except for the Christoffel terms (which do not cancel in this case), the physical strain rate strongly parallels the form for physical vorticity (16).

Assuming a Newtonian fluid, the deviatoric (or viscous) stress in $\mathbf{S}_p$ may be written in the mixed tensor form

$$\rho_b\tau^{*\,j}_{\ \ k} := 2\mu\varepsilon^{*\,j}_{\ \ k} + \lambda v^{*m}_{\ \ ,m}\delta^j_k \ . \tag{41}$$

Here μ and λ are the molecular and bulk viscosities, respectively; the default relationship between the two is set by the Stokes hypothesis. The mixed strain rate tensor $\varepsilon^{*\,j}_{\ \ k}$ may be generated by raising an index on the covariant form given in (40), and $v^{*m}_{\ \ ,m} = -\overline{v}^m\partial\ln(\rho^*)/\partial\overline{x}^m$ from (2). Defining the principle form of deviatoric stress as a mixed tensor comes naturally from the definition relating physical $\rho_b\boldsymbol{\tau}$, total stress $\mathbf{S}$, and pressure; $S^j_k := \rho_b\tau^j_k - p\delta^k_j$.

The viscous force, with components $\mathscr{V}^j$ on the rhs of (3), is proportional to the divergence of the viscous stress tensor $\nabla\bullet(\rho_b\boldsymbol{\tau})$. Since all terms in the momentum equation have the form of acceleration, and the divergence operator consumes one contravariant index with its inner product, then $\rho_b\boldsymbol{\tau}$ must be expressed as a contravariant 2-form. This associated form may be determined from (41) by raising an index. The computation of it's divergence is more complicated than shown earlier in (28), because it requires evaluating covariant derivatives of 2-forms (cf. section 2.5 [31]). The result is:

$$\tau^{*\,jk}_{\ \ \ ,k} = \frac{1}{G}\frac{\partial G\tau^{*\,jk}}{\partial x^k} + \left\{\begin{matrix} j \\ k\ \ p\end{matrix}\right\}\tau^{*kp} \ . \tag{42}$$

In order to determine the coefficient for (42) in $\mathscr{V}^j$ of (3), it is necessary to know the generalized, contravariant form of the momentum equations. In $\mathbf{S}_p$, they take on the form

$$\frac{Dv^{*\,j}}{Dt} := \frac{dv^{*\,j}}{dt} + \left\{\begin{matrix} j \\ p\ \ q\end{matrix}\right\}v^{*p}v^{*q} = \rho_b^{-1}\left(\rho_b\tau^{*\,jk}\right)_{,k} - g^{jk}\pi'_{\ ,k} + \ldots \ , \tag{43}$$

where only the surface forces have been explicitly included on the right hand side. On the extreme left hand side is the material derivative of the contravariant velocity, i.e., the acceleration of the fluid particle in contravariant form. Following the discussion of (46) in section 3.4, the material derivative may be broken apart into a total derivative and Christoffel terms[10]; as is shown in the middle terms of (43). The Christoffel terms are absorbed, after suitable rescaling, into the term $\mathscr{F}^j$ of (3). These terms are apparent Coriolis and centrifugal accelerations, familiar from global geophysical problems. This leaves only the dv^{*j}/dt term on the left hand side of the momentum equation. The physical velocity appearing in (3) may be computed from the contravariant velocity via the rescaling $v^{*j} = \sqrt{g^{jj}}v^j$. Expanding, one finds $dv^{*j}/dt = \sqrt{g^{jj}}\{dv^j/dt + (v^j/\sqrt{g^{jj}})d\sqrt{g^{jj}})/dt\}$. Thus the momentum equation (43) needs to be divided by $\sqrt{g^{jj}}$ (or equivalently, multiplied by $\sqrt{g_{jj}}$ given the orthogonal coordinates of $\mathbf{S}_p$) after rescaling in order to transform it into (3). The terms $(v^j/\sqrt{g^{jj}})d\sqrt{g^{jj}}/dt$, additional apparent accelerations, are absorbed into the $\mathscr{F}^j$ term. In summary, $\mathscr{V}^j = \sqrt{g_{jj}}\rho_b^{-1}(\rho_b\tau^{*jk})_{,k}$. It only remains to (i) transform (42) and the rescaled and reorganized version of (43) from $\mathbf{S}_p$ to $\mathbf{S}_t$ using the chain rule, and (ii) further reorganize terms utilizing the CGL (48) to recover the conservative form for the stress divergence. The details are ommitted here but closely follow previous developments for (21) and (32). Following those manipulations we arrive at

$$\mathscr{V}^j = \frac{1}{\rho^*}\frac{\partial}{\partial \overline{x}^p}\left(\rho^*\widetilde{G}^p_k\sqrt{g_{jj}g_{kk}}\tau^{*jk}\right) - \tau^{*jk}\frac{\partial\sqrt{g_{jj}}}{\partial x^k} + \sqrt{g_{jj}}\left\{\begin{array}{cc} j \\ l & m \end{array}\right\}\tau^{*lm}\,, \tag{44}$$

with

$$\tau^{*jk} = 2\nu g^{jj}g^{kk}\varepsilon^*_{\ jk} + \kappa g^{jk}v^{*m}_{\ \ ,m}\,, \tag{45}$$

where $\nu := \mu/\rho$ is the kinematic viscosity and $\kappa := \lambda/\rho$ is the density normalized bulk viscosity. The last two terms on the rhs of (44) vanish in Cartesian $\mathbf{S}_p$; the first of them arises because we use the physical rather than the contravariant velocity as dependent variable in (3), whereas the second reflects the intrinsic curvilinear nature of $\mathbf{S}_p$.

To illustrate the complete development at work, we highlight the simulation of an idealized stratified rotating flow past a long winding valley. The Froude and Rossby numbers — respective measures of the relative importance of the inertial to buoyancy and Coriolis forces — are both about 0.6, thereby indicating significant nonlinearity of the simulated flow. In spite of the relevance to weather conditions in densely populated areas, this is a poorly understood and unexplored problem — primarily, we believe, because of the lack of adequate mathematical tools. The horizontal model domain in $\mathbf{S}_p$ is bounded by two sinusoids of the same x-wavelength $L_x = 400$ km, separated by constant increment 200 km in y. A cosine-shaped valley with the depth and half-width 0.8 km and 30 km, respectively, is centered in the model domain. The vertical domain is 9 km deep. The ambient wind is $(U,0,0)$ with $U = 5$ m/s, and the buoyancy frequency $N = 0.012$ s^{-1} and relative humidity 92% are assumed (for a discussion of moist thermodynamics and its numerical representation, see [8] and references therein). Boundary conditions are periodic in both horizontal directions. Lower boundary assumes partial slip with typical (for mesoscale simulations) drag coefficient $C_d = 10^{-3}$, and the uniform normal heat flux $H_o = -0.01$ ^{o}Kms^{-1}. The boundary-sink of heat and momentum is felt in the vertical via an arbitrarily specified "eddy viscosity". Its surface value $\nu = \alpha = 0.25\Delta z^2/\Delta t$ is attenuated exponentially to zero with e-folding scale $2\Delta z$. The transformed model domain $\mathbf{S}_t$ is covered with $100\times 50\times 60$ grid increments. The simulation covers 8 h of physical time with $\Delta t = 60$ s. Figure 1 displays the solution after 8 h. The results obtained have been verified against linear estimations, and corresponding 3D/2D simulations on rectangular domains. The benefits of the advocated approach are obvious: the narrower the winding valley, the more prohibitive the cost of standard simulations on rectangular domains. Here, the gain is about a factor of 2.

[10]The reduced range in the lower indices of the Christoffel terms compared to (46) occurs because the coordinates of $\mathbf{S}_p$ are fixed.

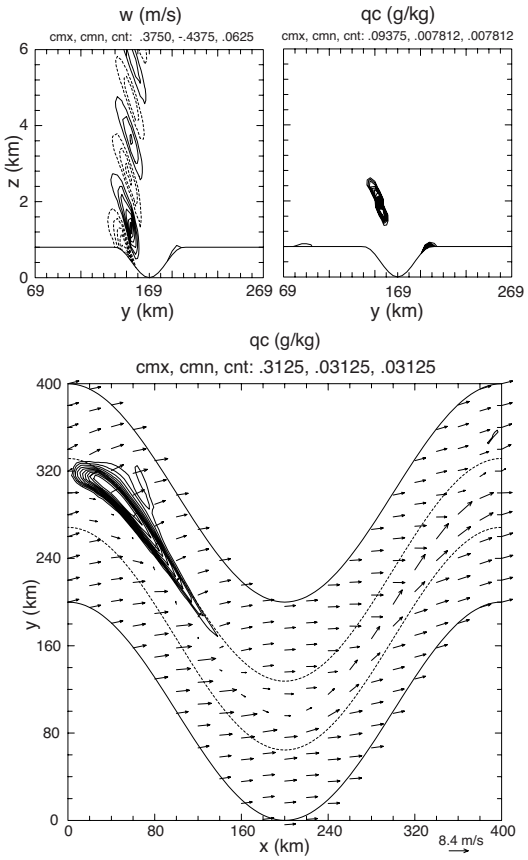

Figure 2: Vertical velocity (outer left panel) and cloud water mixing ratio (inner left panel) in the yz cross section at $x = 120$ km and cloud-water mixing ratio at bottom surface of the model (right panel); two dotted lines along the center of the sinusoidal domain outline the extent of the valley.

3.4 Tensor Identities

Developments discussed in this paper make use of numerous tensor identities and properties. While most have been introduced as needed, here we highlight a few others that we have found particularly useful both for manipulating analytic tensor fields into forms preferred in the numerical model and for evaluating transformation coefficients in the model code[11].

The first identity involves a generalization of the material (also known as substantial) derivative — defined as the time rate of change in fluid property when one follows the flow — to coordinate invariant form. In section 3.2, cf. (31), we noted that for scalar fields the total derivative (defined in section 2.2) is an invariant form and is equivalent to the material derivative. The material derivative of an arbitray tensor field may be constructed by replacing the partial derivatives in (31) with covariant derivatives. In particular, the generalized form of material derivative for the contravariant velocity is:

$$\frac{D\overline{v}^{*j}}{D\bar{t}} := \overline{v}^{*j}_{,m}\overline{v}^{*m} \equiv \frac{d\overline{v}^{*j}}{d\bar{t}} + \overline{\left\{ \begin{array}{cc} j \\ i & m \end{array} \right\}}\overline{v}^{*i}\overline{v}^{*m} \,. \tag{46}$$

Recall that $j = 1,2,3$ whereas $(i,m) = 0,1,2,3$. This expression is not equivalent to the total derivative, hence we use a different notation to distinguish it. More generally, the tensor form (46) is a special case of the *intrinsic* or *absolute* derivative [1] [31].[12] If one wishes to compute the material derivative of a covariant form, then the

[11] For examples, see discussion surrounding Eq.(13) in [34] and the proof of (48) below.

[12] In general the coordinate t can be replaced with the arc length s along any particle path described by $x^j = x^j(s)$; the contravariant velocities being replaced with dx^i/ds.

expression for the covariant derivative of a covariant form (14) would be used in (46) instead of (26). For mixed tensors, additional terms are added to (46) in accord with the covariant and contravariant nature of the tensor (2.516-2.518 in [31]).

The second identity, although elementary, has profound implications for the implementation of the operator calculus in the numerical model. In a four dimensional space, it consists of 16 simultaneous equations — differential identities — that relate the elements of the Jacobi and inverse Jacobi matrices of the transformation defining $\mathbf{S}_t$

$$\delta^i_m \equiv \frac{\partial \overline{x}^i}{\partial x^n}\frac{\partial x^n}{\partial \overline{x}^m} \,. \tag{47}$$

The index n has the range $0,1,2,3$. Given our specified functional form for the transformation, (1), 6 of these reduce to trivial statements (i.e., 0=0 or 1=1), leaving 10 equations relating 20 metric coefficients. Since in our model the problem is solved in $\mathbf{S}_t$, the physical coordinates of $\mathbf{S}_p$ are treated as dependent variables, that is, $x^i = x^i(\overline{x}^m)$. Once the $\partial x^i/\partial \overline{x}^m$ have been determined (either analytically or numerically), the simultaneous equations (47) are used to determine the inverse metric coefficients $\partial \overline{x}^m/\partial x^i$. The use of these differential identities is important for ensuring conservative properties and is deeply embedded in the analytical structure of our numerical model.

The final identity

$$\frac{G}{\overline{G}}\frac{\partial}{\partial \overline{x}^i}\left(\frac{\overline{G}}{G}\frac{\partial \overline{x}^i}{\partial x^m}\right) \equiv 0 \,, \tag{48}$$

is termed the geometric conservation law, or GCL.[13] The left hand side can be recognized as the divergence in $\mathbf{S}_t$ of the contravariant form $(1/G)\partial \overline{x}^i/\partial x^m$ multiplied by the Jacobian of $\mathbf{S}_p$. This contravariant form gives weighted "velocities" ($m = 0$), or "stretching factors" ($m = 1,2,3$) between $\mathbf{S}_p$ and $\mathbf{S}_t$. Evidently (48) is a set of four independent statements about the *conservation of space*; if it is not satisfied, the conservative properties of the numerical model will be lost. Various components of the GCL have been recognized as important in numerical models for 25 years [32].

The easy way to verify the GCL is to begin with any conservation equation written in tensor invariant form. The conservation equation is then transformed from one coordinate system into another using the chain rule, and the resulting expressions are regrouped in order to recover the tensor invariant form. Such an effort will quickly lead to a sole remainder term with a coefficient equal to the left hand side of (48). Only if the GCL is satisfied does this remainder term vanish and the invariant tensor character of the original conservation equation maintained. We have already used the GCL twice in this fashion, while evaluating (i) divergence of vorticity (21), and (ii) scalar advection-diffusion (32).

A proof of (48) via purely geometrical arguments shows the role of tensor identities and transformation laws in maintaining the conservation of space. We begin by setting the left hand side of (48) equal to a residual $\mathscr{R}$ and by direct expansion and tensor manipulations, prove $\mathscr{R} \equiv 0$. Expanding (48) and reorganizing terms yeilds:

$$\mathscr{R} \equiv \left(\frac{1}{\overline{G}}\frac{\partial \overline{G}}{\partial \overline{x}^i}\right)\frac{\partial \overline{x}^i}{\partial x^m} + \frac{\partial x^n}{\partial \overline{x}^i}\frac{\partial}{\partial x^n}\left(\frac{\partial \overline{x}^i}{\partial x^m}\right) - \left(\frac{1}{G}\frac{\partial G}{\partial x^n}\right)\left(\frac{\partial x^n}{\partial \overline{x}^i}\frac{\partial \overline{x}^i}{\partial x^m}\right) \,. \tag{49}$$

In the first term, the parenthetical expression may be replaced with a contracted Christoffel symbol of the second kind in $\mathbf{S}_t$, using (27). In the third term, the derivative of G has been expanded using the chain rule, and regrouped into two parenthetical expressions. The first one can again be rewritten as a contracted Christoffel symbol of the second kind, only now in $\mathbf{S}_p$. The second expression is recognized, via (47), to be a Kronecker

[13] This version of the GCL has been used to derive (2) from the tensor invariant anelastic continuity equation; cf. discussion following (5).

delta function. Clearly n must be set equal to m in this third term. After relabeling dummy (repeating) indices, there results:

$$\mathscr{R} \equiv \overline{\left\{ \begin{array}{cc} n \\ n & i \end{array} \right\}} \frac{\partial \overline{x}^i}{\partial x^m} + \frac{\partial x^n}{\partial \overline{x}^i} \frac{\partial^2 \overline{x}^i}{\partial x^n \partial x^m} - \left\{ \begin{array}{cc} n \\ n & m \end{array} \right\} . \tag{50}$$

The proof is now completed by writing the transformation law for Christoffel symbols of the second kind, and contracting the upper index to one of the lower ones. The details are tedious but standard, resulting in:

$$\left\{ \begin{array}{cc} n \\ n & m \end{array} \right\} \equiv \left(\frac{\partial \overline{x}^o}{\partial x^n} \frac{\partial x^n}{\partial \overline{x}^l} \right) \frac{\partial \overline{x}^i}{\partial x^m} \overline{\left\{ \begin{array}{cc} l \\ o & i \end{array} \right\}} + \frac{\partial x^n}{\partial \overline{x}^o} \frac{\partial^2 \overline{x}^o}{\partial x^n \partial x^m} . \tag{51}$$

The range of indices for l, o is $0, 1, 2, 3$. In the first term on the right, the parenthetical expression is recognized to be another Kronecker delta function, so o must be set equal to l in this term. Then l becomes a dummy index in the transformed Christoffel symbol and may be relabed n. In the second term on the right, o is a dummy index and so may be relabled i. The right hand side of (51) is now recognized to be *exactly* equal to the first two terms on the right hand side of (50) and we have the desired result $\mathscr{R} \equiv 0$, completing the proof.

We observe that establishing the GCL requires the application of the differential identities (47), as well as the use of the transformation rule for Christoffel symbols (51). The former requires that care must be taken in how various metric terms are computed, and the latter that care must be taken in how the derivatives of various metric terms are computed [34]. If these analytical identities are satisfied by the numerical method, then source/sinks will not appear in $\mathscr{R}$, and it will not be necessary to attempt to compensate for this effect by using the components of (48) to generate governing equations for various metric terms such as the Jacobian [32].

4. Remarks

Our approach to developing dynamic grid deformation capability in numerical models is to rigorously implement a continuous mapping from a physical space $\mathbf{S}_p$ where the mathematical model for the problem is originally posed, to a transformed space $\mathbf{S}_t$ where the problem is solved computationally. The reference coordinate system for $\mathbf{S}_p$ may be any fixed orthogonal system, in particular, it can be curvilinear. This represents a significant departure from earlier transformation methods ([7],[33]) which are limited to Cartesian descriptions of $\mathbf{S}_p$; and has required careful rederivation of all relevant physical forms.

While in principle one can always transform from Cartesian coordinates to any other topologically equivalent coordinates, in practice it is easier and more illuminating to use an established reference system that points out the obvious physics, e.g., spherical coordinates for global problems. By limiting $\mathbf{S}_p$ to orthogonal and stationary systems, we take advantage of important simplifications that are unavailable, if for instance, the problem were to be cast in $\mathbf{S}_t$ (which a tensor formulation makes eminently possible). In particular, the scale factors are quite compact, making the computation of the physical forms of the various contravariant and covariant forms that follow much easier. Additionally, the stationary nature of the reference coordinates reduces the index range in many operators.

We also depart from most computational works in emphasizing a tensorial description of the model. Our experience to date is that a tensorial representation is helpful for generating correct and *meaningful* computational forms in arbitrary coordinates. Furthermore, the rules of tensor manipulation and attendant identities provide significant analytical guidance for developing fundamental structure in the core of the numerical model that helps to preserve local as well as global conservation properties in numerous fields ranging from mass balance to the conservation of space itself.

Acknowledgements. This work was supported in part by the Department of Energy "Climate Change Prediction Program" (CCPP) research initiative.

References

[1] Aris R, *Vectors, Tensors, and the Basic Equations of Fluid Mechanics*, Dover Publications, New York, 286 pp. (1989).

[2] Andrews DG, Holton JR, Leovy CB, *Middle Atmosphere Dynamics*, Academic Press, Orlando, 489 pp. (1987).

[3] Clark TL, Farley RD. Severe downslope windstorm calculations in two and three spatial dimensions using anelastic interactive grid nesting: A possible mechanism for gustiness. *J. Atmos. Sci.* 1984; **41**:329–350.

[4] Davis T, Staniforth A, Wood N, Thuburn J. Validity of anelastic and other equation sets as inferred from normal-mode analysis. *Q.J.R. Meteorol. Soc.* 2003; **129**:2761–2775.

[5] Domaradzki JA, Xiao Z, Smolarkiewicz PK. Effective eddy viscosities in implicit large eddy simulations of turbulent flows. *Phys. Fluids* 2003; **15**:3890–3893.

[6] Durran DR, *Numerical Methods for Wave Equations in Geophysical Fluid Dynamics.*, Springer-Verlag; 1999.

[7] Gal-Chen T, Somerville CJ. On the use of a coordinate transformation for the solution of the Navier-Stokes equations. *J. Comput. Phys.* 1975; **17**:209–228.

[8] Grabowski WW, Smolarkiewicz PK. A multiscale anelastic model for meteorological research, *Mon. Weather Rev.* 2002; **130**:939–956.

[9] Lipps FB, Hemler RS. A scale analysis of deep moist convection and some related numerical calculations. *J. Atmos. Sci.* 1982; **39**:2192–2210.

[10] Margolin LG, Shaskhov M, Smolarkiewicz PK. A discrete operator calculus for finite difference approximations. *Comp. Meth. in Appl. Mech. and Engineering* 2000 **187**:365–383.

[11] Margolin LG, Rider WJ. A Rationale for Implicit Turbulence Modeling. *Int. J. Num. Meth. Fluids* 2002; **39**:821–841.

[12] Margolin LG, Smolarkiewicz PK, Wyszogrodzki AA. Implicit turbulence modeling for high Reynolds number flows. *J. Fluids Eng.* 2002; **124**:862–867.

[13] Maurin K. *Analysis Part II: Integration, Distributions, Holomorphic Functions, Tensor and Harmonic Analysis*. Reidel Publishing Co., 1980.

[14] Milne-Thomson LM. *Theoretical Hydrodynamics*. The MacMillan Press Ltd 5th edition, 1968.

[15] R.W. Ogden, *Non-Linear Elastic Deformations*. John Wiley & Sons, pp. 532 (1984).

[16] Oldroyd JG. On the Formulation of Rhelogical Equations of State. *Proc. Roy. Soc.* 1950; **A200**:523-541.

[17] Polavarapu SM, Peltier WR. The Structure and Nonlinear Evolution of Synoptic Scale Cyclones: Life Cycle Simulations with a Cloud-Scale Model. *J. Atmos. Sci.* 1990; **47**:2645-2673.

[18] Prusa JM, Smolarkiewicz PK, Garcia RR. On the propagation and breaking at high altitudes of gravity waves excited by tropospheric forcing. *J. Atmos. Sci.* 1996; **53**:2186–2216.

[19] Prusa JM, Smolarkiewicz PK. An all-scale anelastic model for geophysical flows: dynamic grid deformation. *J. Comput. Phys.* 2003; **190**:601–622.

[20] Randall D, Khairoutdinov M, Arakawa A, Grabowski WW. Breaking the cloud parameterization deadlock. *Bull. Amer. Meteor. Soc.* 2003; **84**:1547-1564.

[21] Rotunno R, Grubišić V, Smolarkiewicz PK, Vorticity and Potential Vorticity in Mountain Wakes. *J. Atmos. Sci.* 1999; **56**:2796–2810.

[22] Smolarkiewicz PK, Grell GA. A class of monotone interpolation schemes. *J. Comput. Phys.* 1992; **101**:431–440.

[23] Smolarkiewicz PK, Pudykiewicz JA. A class of semi-Lagrangian approximations for fluids. *J. Atmos. Sci.* 1992; **49**:2082–2096.

[24] Smolarkiewicz PK, Margolin LG. On forward-in-time differencing for fluids: extension to a curvilinear framework. *Mon. Weather Rev.* 1993; **121**:1847–1859.

[25] Smolarkiewicz PK, Margolin LG. MPDATA: A finite difference solver for geophysical flows. *J. Comput. Phys.* 1998; **140**:459–480.

[26] Smolarkiewicz PK, Margolin LG. Variational methods for elliptic problems in fluid models. *Proc. ECMWF Workshop on Developments in numerical methods for very high resolution global models* 5-7 June 2000; Reading, UK, ECMWF, 137–159.

[27] Smolarkiewicz PK, Margolin LG, Wyszogrodzki AA. A class of nonhydrostatic global models. *J. Atmos. Sci.* 2001; **58**:349–364.

[28] Smolarkiewicz PK, Prusa JM. Forward-in-Time Differencing for Fluids: Simulation of geophysical turbulence. In *Turbulent Flow Computation* Drikakis D, Guertz BJ (eds). Kluwer Academic Publishers, 2002; 207–240.

[29] Smolarkiewicz PK, Prusa JM. Toward mesh adaptivity for geophysical turbulence. *Int. J. Numer. Meth. Fluids* 2004, to appear.

[30] Smolarkiewicz PK, Szmelter J. MPDATA: An Edge-Based Unstructured-Grid Formulation. *J. Comput. Phys.* 2004, submitted.

[31] Synge JL, Schild A. *Tensor Calculus*, Dover Press, 1978.

[32] Thomas PD, Lombard CK. Geometric conservation law and its application to flow computations on moving grids. *AIAA J.* 1979; **17**:1030–1037.

[33] J.F. Thompson, F.C. Thames, and C.W. Mastin. Automatic numerical generation of body-fitted curvilinear coordinate system for field containing any number of arbitrary two-dimensional bodies, *J. Comput. Phys.*, **15**, 299-319 (1974).

[34] Wedi NP, Smolarkiewicz PK. Extending Gal-Chen & Somerville terrain-following coordinate transformation on time-dependent curvilinear boundaries. *J. Comput. Phys.* 2004; **193**:1–20.

[35] Wedi NP, Smolarkiewicz PK. Laboratory for internal gravity-wave dynamics: The numerical equivalent to the quasi-biennial oscillation (QBO) analogue. *Int. J. Numer. Meth. Fluids* 2004, submitted.